A Method for Constructing Solutions of Homogeneous Partial Differential Equations: Localized Waves
Author(s): Rod Donnelly and Richard Ziolkowski
Source: *Proceedings: Mathematical and Physical Sciences*, Vol. 437, No. 1901 (Jun. 8, 1992), pp. 673-692
Published by: The Royal Society
Stable URL: http://www.jstor.org/stable/52134
Accessed: 19/01/2009 14:55

A method for constructing solutions of homogeneous partial differential equations: localized waves

By Rod Donnelly[1] and Richard Ziolkowski[2]

[1] *Faculty of Engineering and Applied Science, Memorial University, St. John's, Newfoundland, Canada A1B 3X5*

[2] *Department of Electrical and Computer Engineering, University of Arizona, Tucson, Arizona 85721, U.S.A.*

We introduce a method for constructing solutions of homogeneous partial differential equations. This method can be used to construct the usual, well-known, separable solutions of the wave equation, but it also easily gives the non-separable localized wave solutions. These solutions exhibit a degree of focusing about the propagation axis that is dependent on a free parameter, and have many important potential applications. The method is based on constructing the space-time Fourier transform of a function so that it satisfies the transformed partial differential equation. We also apply the method to construct localized wave solutions of the wave equation in a lossy infinite medium, and of the Klein–Gordon equation. The localized wave solutions of these three equations differ somewhat, and we discuss these differences. A discussion of the properties of the localized waves, and of experiments to launch them, is included in the Appendix.

1. Introduction

There are various methods of constructing solutions of the homogeneous wave equation in three-dimensional space (see (1) below). If we assume a separable solution in, say, cartesian coordinates, then we might choose plane waves which travel in a particular direction with speed c; in spherical polar coordinates we might choose spherical waves centred on the origin.

Below we introduce a new method for finding both separable and non-separable solutions of constant coefficient homogeneous partial differential equations. We do so by constructing solutions of four well-known homogeneous equations: the free-space wave equation, Laplace's equation, the wave equation in a lossy infinite medium, and the Klein–Gordon equation. The solutions are actually constructed in the spatial and temporal Fourier transform domain. The basic idea is to choose the Fourier transform of the solution as a generalized function which, when multiplied by the transform of the particular differential operator, gives zero in the sense of generalized functions.

In the case of the free-space homogeneous wave equation, we show in §2 how this method easily gives the separable solutions mentioned above. Moreover, we show how the method can be used to construct the interesting, non-separable, localized

Proc. R. Soc. Lond. A (1992) **437**, 673–692
Printed in Great Britain

wave (LW) solution (Ziolkowski 1985, 1989). There is a free parameter in this solution, and the size of this parameter determines the wave–particle nature of the solution. A weighted linear superposition, over the free parameter, of the localized wave solutions is also a solution. We include in §2, rather than in the Appendix, two properties of the localized wave solutions that follow readily from our transform domain representation. We give a simpler derivation of the inequality to be satisfied by the free parameter weighting function (spectrum) in order that the weighted superposition have finite energy, and we also derive the temporal Fourier transform of the localized wave (this is important in launching these waves). We also apply the method to construct a localized wave solution of the two-dimensional free space homogeneous wave equation.

In §3 we briefly construct a solution of the three-dimensional Laplace's equation, valid off the plane $z = 0$, that exhibits a 'focusing' that is dependent on a free parameter.

In §4 we consider the homogeneous wave equation in a lossy infinite medium, and show how to construct localized wave solutions that, apart from a monotonic exponential decay factor with time, behave somewhat similarly to the non-lossy solutions; the difference lies only in a term which affects oscillation along the propagation direction. The Klein–Gordon equation, which we study in §5, also has localized wave solutions, which we construct. Again, the difference between the Klein–Gordon and non-lossy wave equation solutions lies only in a term which affects oscillation along the propagation axis. Both lossy medium and Klein–Gordon solutions exhibit a focusing about the propagation axis which is dependent on a free parameter in the solution.

In §6 we compare the real parts of the non-lossy, lossy medium, and Klein–Gordon localized wave solutions. It is the real parts which are of importance for launching realizations of these solutions. We explain why, although all three solutions exhibit the same degree of focusing about the propagation axis for any value of the free parameter, as the free parameter ranges from zero to infinity the oscillatory natures, along the propagation axis, of the three solutions differ markedly. The value of the free parameter where the oscillatory behaviour changes depends on the conductivity in the lossy medium case, and on the 'mass term' in the Klein–Gordon solution.

In §7 we summarize the general method which we have used in particular to construct localized wave solutions of the homogeneous partial differential equations mentioned above. We indicate how the richness of this method may be used to construct other interesting solutions. Finally, in the Appendix we summarize some of the work done on the localized wave solutions of the homogeneous wave equation, and refer to experiments to launch superpositions of these waves. Their practical potential for application in a wide range of areas, from biomedicine to secure communications, is clear from a study of their properties.

2. Solutions of the homogeneous wave equation

Consider the scalar homogeneous wave equation (HWE) in x, y, z space:

$$\left(\nabla^2 - \frac{1}{c^2}\frac{\partial^2}{\partial t^2}\right)\psi(\boldsymbol{r}, t) = 0, \tag{1}$$

where $\boldsymbol{r} = (x, y, z)$. We shall take a three-dimensional spatial Fourier transform and a one-dimensional temporal Fourier transform of (1). We thus define

$$\mathscr{F}_{\boldsymbol{r},t}\{\psi\}(\boldsymbol{k},\omega) \equiv \mathscr{F}_{\boldsymbol{r}}\mathscr{F}_{t}\{\psi\}(\boldsymbol{k},\omega) = \int_{\mathbb{R}^3} \mathrm{d}\boldsymbol{r} \int_{-\infty}^{\infty} \mathrm{d}t\, \psi(\boldsymbol{r},t)\, \mathrm{e}^{-\mathrm{i}\boldsymbol{k}\cdot\boldsymbol{r}}\, \mathrm{e}^{\mathrm{i}\omega t}. \tag{2}$$

In (2) we denote the vector (k_x, k_y, k_z) of spatial transform variables by $\boldsymbol{k}$, and ω is the temporal transform variable. Equation (1) transforms to

$$(k^2 - \omega^2/c^2)\, \mathscr{F}_{\boldsymbol{r},t}\{\psi\}(\boldsymbol{k},\omega) = 0, \tag{3}$$

where $k = \sqrt{(k_x^2 + k_y^2 + k_z^2)}$.

In the sense of generalized functions, we have the result

$$f(\xi)\, \delta(\xi - \xi_0) = f(\xi_0)\, \delta(\xi - \xi_0), \tag{4}$$

for suitably well-behaved function f, where ξ is an n-dimensional vector variable, and δ denotes the n-dimensional delta function.

With the use of (4) we realize that a solution of (3) is given by

$$\mathscr{F}_{\boldsymbol{r},t}\{\psi\}(\boldsymbol{k},\omega) = \alpha(\omega)\, \delta(k_x)\, \delta(k_y)\, \delta(k_z \pm \omega/c), \tag{5}$$

where α is an arbitrary function, since

$$\begin{aligned}(k^2 - \omega^2/c^2)\, \alpha(\omega)\, \delta(k_x)\, \delta(k_y)\, \delta(k_z \pm \omega/c) \\ = (0 + 0 + \omega^2/c^2 - \omega^2/c^2)\, \alpha(\omega)\, \delta(k_x)\, \delta(k_y)\, \delta(k_z \pm \omega/c) = 0.\end{aligned} \tag{6}$$

The inverse Fourier transform of (5) is given by

$$\begin{aligned}\psi(\boldsymbol{r},t) &= \frac{1}{(2\pi)^4} \int_{\mathbb{R}^3} \mathrm{d}\boldsymbol{k} \int_{-\infty}^{\infty} \mathrm{d}\omega\, [\alpha(\omega)\, \delta(k_x)\, \delta(k_y)\, \delta(k_z \pm \omega/c)]\, \mathrm{e}^{\mathrm{i}\boldsymbol{k}\cdot\boldsymbol{r}}\, \mathrm{e}^{-\mathrm{i}\omega t} \\ &= \frac{1}{(2\pi)^4} \int_{-\infty}^{\infty} \mathrm{d}\omega\, \alpha(\omega)\, \mathrm{e}^{-\mathrm{i}\omega(t \pm z/c)},\end{aligned} \tag{7}$$

which represents a superposition of plane waves, travelling in either the positive or negative z direction, of angular frequency ω. In particular, we can choose $\alpha(\omega) = \delta(\omega - \omega_0)$ and take the negative sign in (5) to get a single plane wave, of frequency ω_0, travelling in the positive z direction.

Another solution of (3) is given by

$$\mathscr{F}_{\boldsymbol{r},t}\{\psi\}(\boldsymbol{k},\omega) = \alpha(\omega)\, \delta(k^2 - \omega^2/c^2). \tag{8}$$

As (8) is spherically symmetric in the spatial transform domain, its inverse transform has spatial spherical symmetry. As k is the distance from the origin in the spatial transform coordinate domain, we have the result that, as generalized functions,

$$\delta(k^2 - \omega^2/c^2) = (1/2k)\, \delta(k - |\omega|/c). \tag{9}$$

To take the inverse Fourier transform of (8) we convert the spatial transform coordinates to spherical polar coordinates. The resulting four-dimensional integral reduces to

$$\psi(\boldsymbol{r},t) = \frac{1}{2\mathrm{i}r(2\pi)^3} \int_{-\infty}^{\infty} \mathrm{d}\omega\, \alpha(\omega)\, \{\exp[-\mathrm{i}\omega(t - r\,\mathrm{sgn}\,(\omega)/c)] - \exp[-\mathrm{i}\omega(t + r\,\mathrm{sgn}\,(\omega)/c)]\}, \tag{10}$$

where $\mathrm{sgn}(\omega) = |\omega|/\omega$. By choosing, say, $\alpha(\omega) = \delta(\omega - \omega_0)$ again, we recover a HWE solution which, for $t > 0$, represents both inward and outward propagating spherical waves, of frequency ω_0.

The method outlined above, and illustrated by the examples of two well-known HWE solutions, can be used systematically to generate other interesting HWE solutions. In particular, we can recover the so-called localized waves (LWs) introduced by Ziolkowski (1985, 1989). These solutions are non-separable, propagate along the z-axis (arbitrarily) at the speed c, and have angular symmetry about the z-axis in a cylindrical (ρ, ϕ, z) coordinate system $(\rho = \sqrt{(x^2+y^2)})$. To this end we note that (3) may be rewritten

$$(\kappa^2 + k_z^2 - \omega^2/c^2)\, \mathscr{F}_{r,t}\{\psi\}(\boldsymbol{k}, \omega) = 0, \tag{11}$$

where $\kappa^2 = k_x^2 + k_y^2$. We shall choose a solution of (11) that constrains the transform variables k_z and ω in such a way as to make the expression $\kappa^2 + k_z^2 - \omega^2/c^2$ vanish. We see that, for example

$$\kappa^2 + (\beta - \kappa^2/4\beta)^2 - (\beta + \kappa^2/4\beta)^2 \equiv 0 \tag{12}$$

for any choice of the arbitrary real non-zero parameter β. As such, any function of the form

$$\Xi(\kappa, \beta)\, \delta[k_z - (\beta - \kappa^2/4\beta)]\, \delta[\omega + c(\beta + \kappa^2/4\beta)], \tag{13}$$

where Ξ is an arbitrary function of κ and β, will satisfy (11). If we specify Ξ by taking

$$\mathscr{F}_{r,t}\{\psi\}(\boldsymbol{k}, \omega) = (\pi^2/\mathrm{i}\beta) \exp(-\kappa^2 z_0/4\beta)\, \delta[k_z - (\beta - \kappa^2/4\beta)]\, \delta[\omega + c(\beta + \kappa^2/4\beta)], \tag{14}$$

where we now assume that $\beta > 0$, and also $z_0 > 0$ is arbitrary, then we can apply an inverse Fourier transform to get

$$\psi(\boldsymbol{r}, t) = \frac{\pi^2}{\mathrm{i}\beta(2\pi)^4} \mathrm{e}^{\mathrm{i}\beta(z+ct)} \int_{\mathbb{R}^2} \mathrm{d}\boldsymbol{\kappa}\, \mathrm{e}^{-\mathrm{i}\boldsymbol{\kappa}\cdot\boldsymbol{\pi}} \exp\{-\kappa^2[z_0 + \mathrm{i}(z-ct)]/4\beta\}. \tag{15}$$

In (15), $\boldsymbol{\kappa}\cdot\boldsymbol{\rho} = k_x x + k_y y$; we are free to choose the k_x-axis as lying in the direction of $\boldsymbol{\rho}$, so that $\int_{\mathbb{R}^2} \mathrm{d}\boldsymbol{\kappa}\, \mathrm{e}^{-\mathrm{i}\boldsymbol{\kappa}\cdot\boldsymbol{\rho}}$ reduces to

$$\int_0^\infty \mathrm{d}\kappa \int_0^{2\pi} \mathrm{d}\varphi\, \mathrm{e}^{-\mathrm{i}\kappa\rho\cos\varphi}.$$

The angular integral can be recognized as a zero-order Bessel function. Thus,

$$\psi(\boldsymbol{r}, t) = \frac{\pi^2}{\mathrm{i}\beta(2\pi)^3} \mathrm{e}^{\mathrm{i}\beta(z+ct)} \int_0^\infty \mathrm{d}\kappa\, \kappa J_0(\kappa\rho) \exp\{-\kappa^2[z_0 + \mathrm{i}(z-ct)]/4\beta\}. \tag{16}$$

Finally, the integral in κ may be evaluated (Gradshteyn & Ryzhik 1980, result 6.631.4) to give

$$\psi(\boldsymbol{r}, t) = \mathrm{e}^{\mathrm{i}\beta(z+ct)} \frac{\exp\{-\rho^2\beta/[z_0 + \mathrm{i}(z-ct)]\}}{4\pi\mathrm{i}[z_0 + \mathrm{i}(z-ct)]}. \tag{17}$$

The function given in (17) represents, for arbitrary positive z_0 and β, the generic LW as mentioned above. It has some fascinating properties, which we describe in the Appendix, together with a brief summary of results from acoustic experiments to launch superpositions of LWs.

From the steps leading from (11) to (17), we see how 'natural' the LW solutions seem when viewed in light of the constraints on the transform domain variables k_z

and ω. Indeed, it can be verified that the constraints implied by (12) and (13) represent the simplest nontrivial ones on k_z and ω. It should be pointed out that this 'forcing' of the wave operator in the transform domain, $k^2-\omega^2/c^2$, is akin to the factorization of the wave operator $\nabla^2-(1/c^2)\,\partial/\partial t^2$ as given in Besieris *et al.* (1989).

It is of some interest to determine the temporal Fourier transform of the generic LW in (17). This has not been given previously. The temporal transform should be of use when designing schemes to launch superpositions of the LWS (Ziolkowski *et al.* 1989). It cannot easily be found directly from (17), but rather, we shall take an inverse three-dimensional spatial Fourier transform of the result (14). An inverse z Fourier transform gives

$$\mathscr{F}_{x,y,t}\{\psi\}(k_x,k_y,z,\omega)=(\pi/2\mathrm{i}\beta)\exp(-\kappa^2 z_0/4\beta)\exp[\mathrm{i}z(\beta-\kappa^2/4\beta)]\,\delta[(\omega+c\beta)+c\kappa^2/4\beta]. \tag{18}$$

We see clearly that the delta function equals zero if $\omega > -c\beta$. We can show that, as generalized functions,

$$\delta(-b_1^2+b_2^2\kappa^2)=(1/2|b_1 b_2|)\,\delta(\kappa-|b_1|/|b_2|), \tag{19}$$

provided $b_1 \neq 0$ and $b_2 \neq 0$. Using this result we can take the inverse two-dimensional spatial Fourier transform of (18), assuming that $\omega+c\beta<0$:

$$\mathscr{F}_t\{\psi\}(\omega)=\frac{\pi}{(2\pi)^2\,\mathrm{i}c}\exp[\omega(z_0+\mathrm{i}z)/c]\exp[\beta(z_0+2\mathrm{i}z)]\int_0^{2\pi}\mathrm{d}\varphi \times\exp[\mathrm{i}\rho\cos\varphi\sqrt{(4\beta|\omega+c\beta|/c)}]. \tag{20}$$

That is,

$$\mathscr{F}_t\{\psi\}(\omega)=\begin{cases}(1/2\mathrm{i}c)\exp[\omega(z_0+\mathrm{i}z)/c]\exp[\beta(z_0+2\mathrm{i}z)]J_0(\rho\sqrt{(4\beta|w+c\beta|/c)}), & \text{if } \omega<-c\beta\\ 0 & \text{if } \omega>c\beta.\end{cases} \tag{21}$$

As $\mathscr{F}_t\{\psi^*\}(\omega)=(\mathscr{F}_t\{\psi\}(-\omega))^*$, where the asterisk superscript denotes complex conjugation, we see that $\mathscr{F}_t\{\mathscr{R}e(\psi)\}(\omega)$ will contain no temporal frequencies in the range $(-c\beta,c\beta)$. On the z-axis ($\rho=0$), $|\mathscr{F}_t(\psi\}(\omega)|$ is independent of z and decays as $\mathrm{e}^{\omega z_0}$ for $\omega<-c\beta$. The parameter β determines the wave–particle nature of $\psi(\boldsymbol{r},t)$ in (17), depending on whether it is small or large, as has been pointed out in Ziolkowski (1985, 1989). Off the z-axis, for any z, the decay of $|\mathscr{F}_t\{\psi\}(\omega)|$ is further enhanced by the term $|J_0(\rho\sqrt{(4\beta|\omega+c\beta|/c)})|$; in this case the fall off in the magnitude of any fixed temporal frequency component increases with increasing ρ and/or β.

As pointed out (Ziolkowski 1985, 1989), appropriate superpositions of generic LWS of the form (17), for different values of the parameter β, also represent solutions of the HWE. That is

$$f(\boldsymbol{r},t)=\int_0^\infty \mathrm{d}\beta\,\psi_\beta(\boldsymbol{r},t)\,F(\beta), \tag{22}$$

is also a solution of the HWE, where ψ_β has now been used to denote the function previously called ψ in (17). The spatio-temporal Fourier transform of the expression in (22) is

$$\mathscr{F}_{r,t}\{f\}(\boldsymbol{k},\omega)=\frac{\pi^2}{\mathrm{i}}\int_0^\infty \mathrm{d}\beta\frac{F(\beta)}{\beta}\exp\left(-\frac{\kappa^2 z_0}{4\beta}\right)\delta\left[k_z-\left(\beta-\frac{\kappa^2}{4\beta}\right)\right]\delta\left[\omega+c\left(\beta+\frac{\kappa^2}{4\beta}\right)\right], \tag{23}$$

and indeed this function of $\boldsymbol{k}$ and ω still satisfies (3).

The total energy $\mathscr{E}$, of a scalar wave field, $f(\boldsymbol{r},t)$, can be represented as

$$\mathscr{E} = \int_{\mathbb{R}^3} \mathrm{d}\boldsymbol{r}|f(\boldsymbol{r},t)|^2, \tag{24}$$

and it is not difficult to see that if the scalar wave field consists of a single generic LW with, say, parameter β_0 (put $F(\beta) = \delta(\beta-\beta_0)$ in (22)), then this $\mathscr{E}$ is infinite. However, as pointed out (Ziolkowski 1985, 1989), the spectral weighting term $F(\beta)$ in (22) can be chosen so as to cause the $\mathscr{E}$ in (24) to be finite. This situation is akin to that in the classical Fourier plane wave decomposition of a scalar wave field, wherein each plane wave has infinite energy. A bound on $F(\beta)$ in (22), so that the $\mathscr{E}$ in (24) remains finite, has been given (Ziolkowski 1989). We shall obtain this bound in a somewhat more straightforward way. Using Parseval's theorem, we may rewrite (24)

$$\mathscr{E} = \frac{1}{(2\pi)^3}\int_{\mathbb{R}^3} \mathrm{d}\boldsymbol{k}|\mathscr{F}_r\{f\}(\boldsymbol{k},t)|^2. \tag{25}$$

From (23) we have

$$\mathscr{F}_r(\boldsymbol{k},t) = \frac{\pi}{2\mathrm{i}}\int_0^\infty \mathrm{d}\beta \frac{F(\beta)}{\beta}\exp\left(\frac{-\kappa^2 z_0}{4\beta}\right)\delta\left[k_z-\left(\beta-\frac{\kappa^2}{4\beta}\right)\right]\exp\left[\left(\mathrm{i}tc\frac{\beta+\kappa^2}{4\beta}\right)\right] \tag{26}$$

and so we may write

$$\begin{aligned}\frac{1}{(2\pi)^3}\int_{\mathbb{R}^3} \mathrm{d}\boldsymbol{k}|\mathscr{F}_r\{f\}(\boldsymbol{k},t)|^2 \leqslant \frac{1}{16\pi}\int_{\mathbb{R}^3}\mathrm{d}\boldsymbol{k}\int_0^\infty \mathrm{d}\beta\frac{|F(\beta)|}{\beta}\exp\left(-\frac{\kappa^2 z_0}{4\beta}\right)\delta\left[k_z-\left(\beta-\frac{\kappa^2}{4\beta}\right)\right]\\ \times\int_0^\infty \mathrm{d}\beta'\frac{|F(\beta')|}{\beta'}\exp\left(-\frac{\kappa^2 z_0}{4\beta'}\right)\delta\left[k_z-\left(\beta'-\frac{\kappa^2}{4\beta'}\right)\right].\end{aligned} \tag{27}$$

If we make the changes of variables $\beta-\kappa^2/4\beta = \xi$ and $\beta'-\kappa^2/4\beta' = \eta$ in the second and third integrals, respectively, on the right in (27), we find

$$\begin{aligned}\mathscr{E} \leqslant \frac{1}{16\pi}\int_{\mathbb{R}^3}\mathrm{d}\boldsymbol{k}\int_{-\infty}^\infty \frac{\mathrm{d}\xi}{\sqrt{(\xi^2+\kappa^2)}}|F(\tfrac{1}{2}(\xi+\sqrt{(\xi^2+\kappa^2)}))|\exp\left[-\frac{\kappa^2 z_0}{2(\xi+\sqrt{(\xi^2+\kappa^2)})}\right]\delta(k_z+\xi)\\ \times\int_{-\infty}^\infty \frac{\mathrm{d}\eta}{\sqrt{(\eta^2+\kappa^2)}}|F(\tfrac{1}{2}(\eta+\sqrt{(\eta^2+\kappa^2)}))|\exp\left[-\frac{\kappa^2 z_0}{2(\eta+\sqrt{(\eta^2+\kappa^2)})}\right]\delta(k_z+\eta).\end{aligned} \tag{28}$$

In (28) the integral over k_z represents the convolution of two delta functions, and so it reduces to $\delta(\eta-\xi)$. The integral with respect to, say, η may then be performed to give

$$\mathscr{E} \leqslant \frac{1}{16\pi}\int_{\mathbb{R}^2}\mathrm{d}\boldsymbol{\kappa}\int_{-\infty}^\infty \frac{\mathrm{d}\xi}{\xi^2+\kappa^2}|F(\tfrac{1}{2}(\xi+\sqrt{(\xi^2+\kappa^2)}))|^2\exp\left[-\frac{\kappa^2 z_0}{(\xi+\sqrt{(\xi^2+\kappa^2)})}\right]. \tag{29}$$

We now make the 'inverse' change of variable $\beta-\kappa^2/4\beta = \xi$, so that $\beta = \frac{1}{2}(\xi+\sqrt{(\xi^2+\kappa^2)})$ and so

$$\begin{aligned}\mathscr{E} &\leqslant \frac{1}{16\pi}\int_{\mathbb{R}^2}\mathrm{d}\boldsymbol{\kappa}\int_0^\infty \mathrm{d}\beta\frac{|F(\beta)|^2}{\beta^2}\exp\left(-\frac{\kappa^2 z_0}{2\beta}\right)\\ &= \frac{1}{8z_0}\int_0^\infty \mathrm{d}\beta\frac{|F(\beta)|^2}{\beta}.\end{aligned} \tag{30}$$

Thus the scalar field consisting of superposition of LWs, as given in (22), will have finite total energy if

$$\int_0^\infty \mathrm{d}\beta\, |F(\beta)|^2/\beta < \infty,$$

provided $z_0 > 0$. If $z_0 = 0$ then the generic LW in (17) loses its significant characteristic of exponential decay perpendicular to the z-axis, and we are not dealing with a true LW any more.

We can parallel the above analysis to show the existence of LW solutions of the two-dimensional HWE. These solutions are of practical interest, for example, in waveguide modes of propagation. If we apply a two-dimensional spatial and one-dimensional temporal Fourier transform to the equation

$$\left(\frac{\partial^2}{\partial x^2}+\frac{\partial^2}{\partial y^2}-\frac{1}{c^2}\frac{\partial^2}{\partial t^2}\right)\psi(x,z,t) = 0, \tag{31}$$

we get

$$(k_x^2+k_z^2-\omega^2/c^2)\,\mathscr{F}_{x,z,t}\{\psi\}\,(k_x,k_z,\omega) = 0. \tag{32}$$

Equation (32) admits as a solution

$$\mathscr{F}x,z,t\{\psi_\beta\}\,(k_x,k_z,\omega) = \alpha\exp\,(-k_x^2 z_0/4\beta)\,\delta[k_z-(\beta-k_x^2/4\beta)]\,\delta[\omega+c(\beta+k_x^2/4\beta)], \tag{33}$$

where α is an arbitrary constant, and $z_0 > 0$. If we choose $\alpha = 2\pi^3/2\sqrt{(\pi\beta)}$, we find that

$$\psi_\beta(x,z,t) = \mathrm{e}^{\mathrm{i}\beta(z+ct)}\exp\{-\beta x^2/[z_0+\mathrm{i}(z-ct)]\}/\sqrt{(z_0+\mathrm{i}(z-ct))}\,. \tag{34}$$

The solution (34) of the two-dimensional HWE shares properties with the LW solution (14) of the three-dimensional HWE. In particular, we can also form superpositions

$$\int_0^\infty \mathrm{d}\beta\,\psi_\beta(x,z,t)\,F(\beta),$$

for ψ_β as given in (34), which will also be a solution of the two-dimensional HWE.

Again, of practical interest for launching superpositions of (34), we should like to know the temporal Fourier transforms of the solution. If we apply an inverse two-dimensional spatial Fourier transform to (33) we obtain,

$$\mathscr{F}_t\{\psi_\beta\}\,(x,z,\omega) = \begin{cases} \dfrac{2\cos\,(x\sqrt{(4\beta|\omega+c\beta|/c)})}{\sqrt{(c|\omega+c\beta|/\pi)}}\exp\,[\omega(z_0+\mathrm{i}z)/c]\exp\,[\beta(z_0+2\mathrm{i}z)], & \text{if } \omega < -c\beta, \\ 0, & \text{if } \omega > -c\beta. \end{cases} \tag{35}$$

We note the singular nature of $\mathscr{F}_t\{\psi_\beta\}\,(x,z,\omega)$ (albeit integrable with respect to β) as $\omega \to -(c\beta)_-$ in (37). The temporal Fourier transform in (35), as compared with (21), is somewhat simpler. In particular, because of the J_0 appearing in the latter, the temporal Fourier transform of the so-called 'modified power spectrum' (MPS) solution (resulting from a particular choice of $F(\beta)$ in (22) (Ziolkowski 1989)) cannot be found exactly, except for $\rho = 0$. This is somewhat of a nuisance when designing means to launch acoustic realizations of these three-dimensional superpositions. The trigonometric term appearing in (35) should alleviate this problem.

3. Solutions of Laplace's equation in three dimensions

We can apply the above method to find interesting solutions of Laplace's equation. If we apply a three-dimensional spatial Fourier transform to

$$\nabla^2\psi(\boldsymbol{r}) = 0, \tag{36}$$

we get

$$(k_x^2+k_y^2+k_z^2)\,\mathscr{F}_r\{\psi\}(\boldsymbol{k}) = 0 \tag{37}$$

We see that

$$k_x^2+(\beta-k_x^2/4\beta)^2-(\beta+k_x^2/4\beta)^2 \equiv 0, \tag{38}$$

and this suggests a solution of the form

$$\mathscr{F}_r\{\psi_\beta\}(\boldsymbol{k}) = \Xi(k_x)\,\delta[k_y+(\beta+k_x^2/4\beta)]\{\delta[k_z+\mathrm{i}(\beta+k_x^2/4\beta)]+\delta[k_z-\mathrm{i}(\beta+k_x^2/4\beta)]\}. \tag{39}$$

If we choose $\Xi(k_x) = a\exp(-k_x^2 z_0/4\beta)$, with $z_0 > 0$ and $a = (2\pi)^2\sqrt{(\pi/\beta)}$, then the inverse z Fourier transform exists only if $|z| > 0$. We get

$$\psi_\beta(\boldsymbol{r}) = \mathrm{e}^{-\beta(|z|+\mathrm{i}y)}\frac{\exp[-\beta x^2/(z_0+|z|-\mathrm{i}y)]}{\sqrt{(z_0+|z|-\mathrm{i}y)}}, \quad \text{if } |z| > 0, \tag{40}$$

where we choose the branch cut of the square root function to lie along the negative real axis. It is readily verified that (40) is indeed a solution of Laplace's equation in the region $|z| > 0$.

4. Solutions of the HWE in lossy media

We apply the above method to show that lightly modified LW solutions exist for the equation governing wave motion in a lossy medium having permittivity ϵ, permeability μ, and conductivity σ (all assumed to be constants):

$$\left\{\nabla^2-\epsilon\mu\frac{\partial^2}{\partial t^2}-\mu\sigma\frac{\partial}{\partial t}\right\}\psi(\boldsymbol{r},t) = 0. \tag{41}$$

Applying a three-dimensional spatial and a one-dimensional temporal Fourier transform to (41) results in

$$(\kappa^2+k_z^2-\omega^2/c^2-\mathrm{i}\gamma\omega)\,\mathscr{F}_{r,t}\{\psi\}(\boldsymbol{k},\omega) = 0, \tag{42}$$

where $c^2 = 1/\epsilon\mu$ and $\gamma = \mu\sigma$. With the *a priori* expectation of a solution that decays with time, throughout space, we consider the following transform domain function:

$$\mathscr{F}_{r,t}\{\psi_\beta\}(\boldsymbol{k},\omega) = \Xi(\kappa)\,\delta[k_z+(p_1-\kappa^2/4\beta)]\,\delta[\omega-c(\mathrm{i}b-(p_2+\kappa^2/4\beta))]. \tag{43}$$

In (43), we assume that $\beta > 0$, $\Xi(\kappa)$ is arbitrary, and that p_1, p_2 and b are, as yet, unspecified real parameters. Substituting this function in the left-hand side of (42), and collecting real and imaginary coefficients of κ^2 and κ^0, we get

$$\{\kappa^2[1-p_1/2\beta-p_2/2\beta]+\mathrm{i}\kappa^2[b/2\beta+\gamma c/4\beta]+[p_1^2+b^2-p_2^2+\gamma cb] +\mathrm{i}[2bp_2+\gamma cp_2]\}\mathscr{F}_{r,t}\{\psi_\beta\}(\boldsymbol{k},\omega). \tag{44}$$

Thus the function (43) will represent a solution of (42) if the following constraints are met:

$$\left.\begin{aligned}&\text{(i)}\ \ p_1+p_2 = 2\beta;\\ &\text{(ii)}\ \ b = -\gamma c/2;\\ &\text{(iii)}\ \ p_1^2-p_2^2 = b^2.\end{aligned}\right\} \tag{45}$$

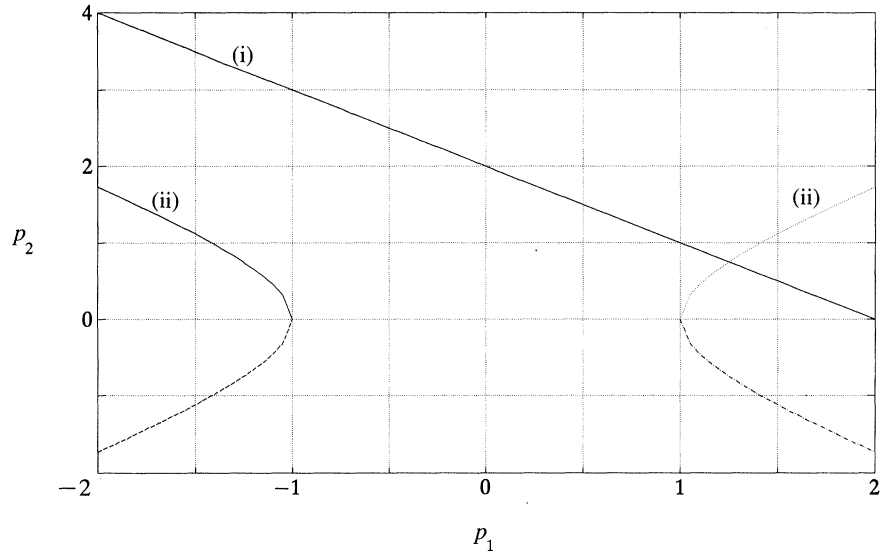

Figure 1. Parameter constraints on lossy medium wave equation LW solution, shown plotted for $|b| = 1$ and $\beta = 1$. (i) $p_1 + p_2 = 2\beta$; (ii) $p_1^2 - p_2^2 = b^2$.

We may demonstrate constraints (i) and (iii) graphically. Referring to figure 1 we see that, for any value of $\beta > 0$, we have the unique solutions

$$p_1 = \beta + b^2/4\beta, \quad p_2 = \beta - b^2/4\beta. \tag{46}$$

We note that, for $\beta < \frac{1}{2}|b| \equiv \frac{1}{4}\mu\sigma c$, p_2 becomes negative. In any case, with the above constraints, (43) is a solution of (42), and $\beta > 0$ is the only free parameter. We may apply inverse z and t Fourier transforms to (43) to get

$$\mathscr{F}_{x,y}\{\psi_\beta\}(\kappa, z, t) = \begin{cases} -(\Xi(\kappa)/(2\pi)^2)\exp[\mathrm{i}z(p_1 - \kappa^2/4\beta)]\exp[-\mathrm{i}ct(\mathrm{i}b - (p_2 + \kappa^2/4\beta))], \\ \qquad\qquad\qquad\qquad\qquad\qquad\qquad\qquad\qquad\qquad \text{if } t > 0; \\ 0, \text{ if } t < 0. \qquad\qquad\qquad\qquad\qquad\qquad\qquad\qquad\qquad\qquad \text{if } t > 0; \end{cases} \tag{47}$$

Finally, if we choose $\Xi(\kappa) = -a\exp(-\kappa^2 z_0/4\beta)$, where $z_0 > 0$ and $a = (2\pi)^3/2\beta$, we can apply inverse x and y Fourier transforms to (46) to get

$$\psi_\beta(\rho, z, t) = \mathrm{e}^{-ct|b|}\exp[\mathrm{i}(zp_1 + ctp_2)]\exp\{-\beta\rho^2/[z_0 + \mathrm{i}(z - ct)]\}/[z_0 + \mathrm{i}(z - ct)] \tag{48}$$

as a solution, for $t > 0$ of the lossy medium wave equation (41), where p_1, p_2 and b are fixed through (44).

The lossy medium LW solution (47) may be compared with the non-lossy solution in (17). Aside from the damping factor, $\mathrm{e}^{-ct|b|}$, (47) differs from (17) in that the term $\exp[\mathrm{i}(zp_1 + ctp_2)]$ can represent the modulation of the remaining term by a plane wave that travels either in the negative or positive z direction, depending on whether $\beta > \frac{1}{2}|b|$ or $\beta < \frac{1}{2}|b|$. Regarding this modulating plane wave, we see that $p_1/2\pi$, corresponding to the wave number (i.e. number of waves per unit distance) is a non-monotonic positive function of β. From (45) we see that p_1 has a minimum (of $|b|$) when $\beta = \frac{1}{2}|b|$, and it is precisely this value of β which sets $p_2 = 0$. At this value of β the modulating plane wave becomes stationary in time, with harmonic oscillations

along the z axis of propagation. The modulating plane wave has a phase velocity of cp_2/p_1 units per second, and tends to $-c$ as $\beta \to 0$, is zero for $\beta = \frac{1}{2}|b|$, and tends to $+c$ as $\beta \to \infty$. On the other hand, the modulating plane wave $e^{i\beta(z+ct)}$ in (17) has a monotone increasing wave number, $\beta/2\pi$, and a constant phase velocity c in the negative z direction. In both solutions the envelope (magnitude) of the solution travels with speed c in the positive z direction.

We note that, as $\sigma \to 0$, $b \to 0$, p_1 and $p_2 \to \beta$ and the lossy solution (47) reduces to the non-lossy LW (17), apart from constants. Thus the original LW is recovered for vanishing conductivity.

5. Solutions of the Klein–Gordon equation

Consider the Klein–Gordon equation:

$$\left\{\frac{1}{c^2}\frac{\partial^2}{\partial t^2} - \nabla^2 + \mu^2\right\}\psi(\boldsymbol{r}, t) = 0. \tag{49}$$

If we apply a three-dimensional spatial and a one-dimensional temporal Fourier transform to (48) we get

$$\{\kappa^2 + k_z^2 - \omega^2/c^2 + \mu^2\}\,\mathscr{F}_{r,t}\{\psi\}(\boldsymbol{k}, \omega) = 0. \tag{50}$$

Consider a transform domain function of the form

$$\mathscr{F}_{r,t}\{\psi_\beta\}(\boldsymbol{k}, \omega) = \Xi(\kappa)\,\delta[k_z + (p_1 - \kappa^2/4\beta)]\,\delta[\omega + c(p_2 + \kappa^2/4\beta)], \tag{51}$$

where, again, we assume that $\beta > 0$, $\Xi(\kappa)$ is arbitrary, and that p_1 and p_2 are, as yet, unspecified real parameters. Substituting the function (50) in the left-hand side of (49), and collecting coefficients of κ^2 and κ^0, we get

$$\{\kappa^2[1 - p_1/2\beta - p_2/2\beta] + [p_1^2 - p_2^2 + \mu^2]\}\,\mathscr{F}_{r,t}\{\psi_\beta\}(\boldsymbol{k}, \omega). \tag{52}$$

Thus, (50) will represent a solution of (49) if the following constraints are met:

$$\left.\begin{aligned} &\text{(i)}\ \ p_1 + p_2 = 2\beta; \\ &\text{(ii)}\ \ p_2^2 - p_1^2 = \mu^2. \end{aligned}\right\} \tag{53}$$

The constraints in (52) are shown graphically in figure 2. For any value of $\beta > 0$ we have the unique solutions

$$p_1 = \beta - \mu^2/4\beta, \quad p_2 = \beta + \mu^2/4\beta. \tag{54}$$

For $\beta < \frac{1}{2}|\mu|$, p_1 is negative. If we choose $\Xi(\kappa) = a\exp(-\kappa^2 z_0/4\beta)$, where $a = (2\pi)^3/2\beta$, we find from (50) that

$$\psi_\beta(\rho, z, t) = \exp[\mathrm{i}(zp_1 + ctp_2)]\exp\{-\beta\rho^2/[z_0 + \mathrm{i}(z - ct)]\}/[z_0 + \mathrm{i}(z - ct)] \tag{55}$$

is a solution of the Klein–Gordon equation (48), for any $\beta > 0$, with p_1 and p_2 given in (53).

Comparing (54) with the original LW solution in (17), we see that in (54) the term representing the modulating plane wave, $\exp[\mathrm{i}(zp_1 + ctp_2)]$, can travel in either the negative or positive z direction, depending on whether $\beta > \frac{1}{2}|\mu|$ or $\beta < \frac{1}{2}|\mu|$,

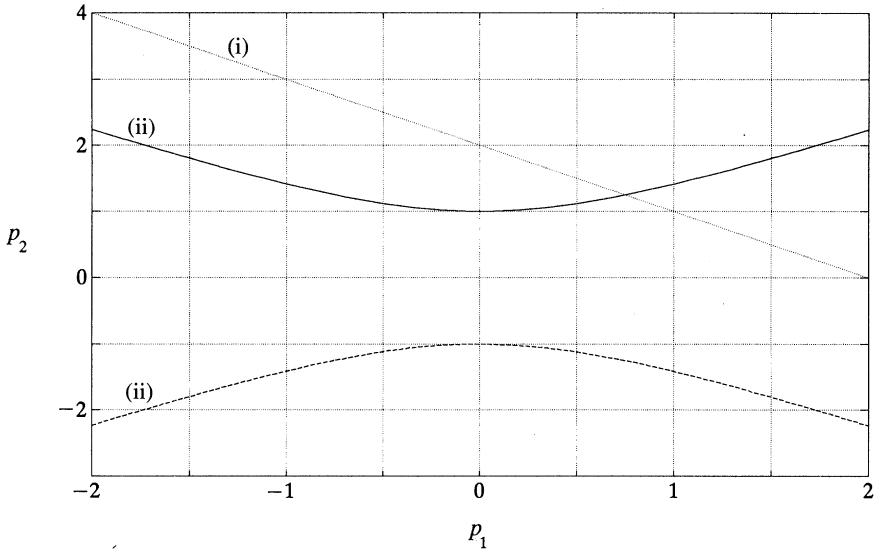

Figure 2. Parameter constraints on Klein–Gordon equation LW solution, shown plotted for $\mu = 1$ and $\beta = 1$. (i) $p_1 + p_2 = 2\beta$; (ii) $p_2^2 - p_1^2 = \mu^2$.

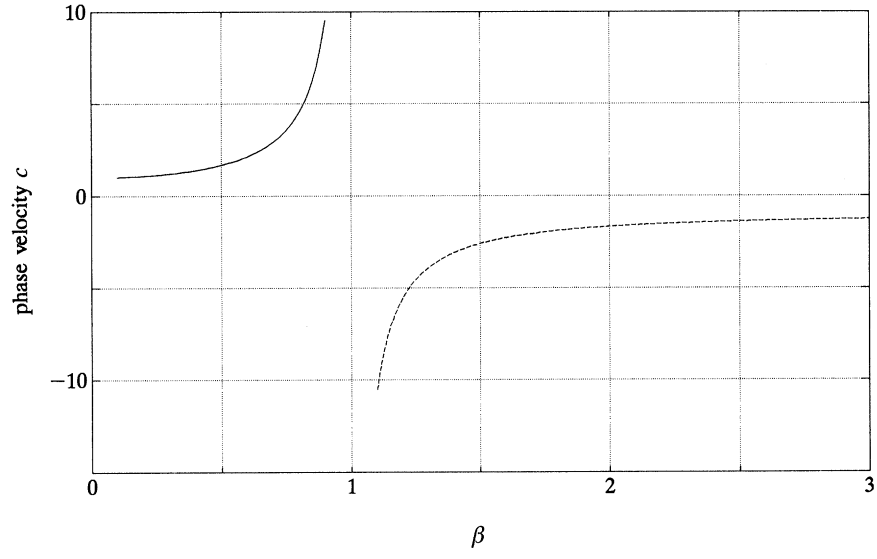

Figure 3. Phase velocity/c as a function of β for the plane wave term in the Klein–Gordon LW solution, valid for $\mu = 2$.

respectively. As noted in §4, the term representing the modulating plane wave in (17), $e^{i\beta(z+ct)}$, travels only in the negative z-direction, with wave number $\beta/2\pi$ and speed c. The modulating plane wave term in (54) has a wave number $|p_1|/2\pi$, which is zero if $\beta = \frac{1}{2}|\mu|$; this results in a standing wave modulation $e^{ict|\mu|}$. The phase velocity of the plane wave, in the positive z direction, in (54) is $-cp_2/p_1 \equiv -c(4\beta^2+\mu^2)/(4\beta^2-\mu^2)$. As seen from figure 3, as $\beta \to 0_+$, this phase velocity tends to c, but as $\beta \to \mu_-$, the phase velocity tends to infinity. As $\beta \to \infty$ the phase velocity approaches $-c$, but as $\beta \to \mu_+$, the phase velocity approaches minus infinity. For all

positive β we have $c|p_2/p_1| > c$. Thus, as the wave number approaches zero, the phase velocity of the modulating plane wave becomes unbounded. The envelope (magnitude) of the Klein–Gordon solution (54), for all β, travels with constant speed c in the positive z direction.

6. Comparison of the time varying solutions

An explanation of the differences between the homogeneous wave equation, lossy medium wave equation, and Klein–Gordon equation localized wave solutions (which we shall label $\psi_{\beta\text{HWE}}$, $\psi_{\beta\text{LMWE}}$, and $\psi_{\beta\text{KGE}}$, respectively) is straightforward. For comparison purposes we shall neglect the arbitrary factor of $4\pi\text{i}$ in the denominator of $\psi_{\beta\text{HWE}}$ in (17) (which was only included to show agreement with the original reference), and also the decay factor, $\text{e}^{-c\epsilon|b|}$, in the $\psi_{\beta\text{LMWE}}$ solution. For purposes of launching realizations of these solutions we need be concerned only with their real parts. We shall explain the spatial distributions of the real parts of these solutions for fixed time, t (in figures 4, 5 and 6 we choose $t = 0$). For this purpose it suffices to consider the solutions for $\rho = 0$ and $t = 0$; we see from (17), (50), and (57) that the decay perpendicular to the z-axis is the same for all three solutions. From (17), (50) and (57) then, neglecting the effects mentioned above, we have

$$\text{Re}\{\psi_{\beta\text{HWE}}(0, z, 0)\} = \text{Re}\left\{\frac{\text{e}^{\text{i}\beta z}}{z_0 + \text{i}z}\right\}, \tag{56}$$

$$\text{Re}\{\psi_{\beta\text{LMWE}}(0, z, 0)\} = \text{Re}\left\{\frac{\exp[\text{i}z(\beta + b^2/4\beta)]}{z_0 + \text{i}z}\right\}, \tag{57}$$

$$\text{Re}\{\psi_{\beta\text{KGE}}(0, z, 0)\} = \text{Re}\left\{\frac{\exp[\text{i}z(\beta - \mu^2/4\beta)]}{z_0 + \text{i}z}\right\}, \tag{58}$$

where $b = -\frac{1}{2}\gamma c = -\sigma\sqrt{(\mu/\epsilon)}$, from (45), and the μ (permeability) term in b should not be confused with the μ (mass) in the Klein–Gordon solution. For fixed b and μ (say, conductivity in the lossy medium, and mass in Klein–Gordon equation, respectively) we see that for large β, the terms $\exp(-\text{i}zb^2/4\beta)$ and $\exp(\text{i}z\mu^2/4\beta)$ will contribute very slow oscillations to (57) and (58) as z varies, as compared with the term $\text{e}^{\text{i}z\beta}$, which is common to all three solutions. If β is very small, the terms $\exp(\text{i}zb^2/4\beta)$ and $\exp(-\text{i}z\mu^2/4\beta)$ will contribute very rapid oscillations, as z varies, to the solutions (57) and (58), respectively. Thus for large β we expect (56), (57) and (58) to look similar, whereas for small β we expect (57) and (58) to oscillate more rapidly, as z varies, than does (56). Note, however, that for the value $\beta = \frac{1}{2}\mu$ there is no oscillatory term in the $\psi_{\beta\text{KGE}}$ solution, (58).

The approximate cut-offs for 'large' and 'small' β oscillatory behaviour can be chosen from plots of the functions β, $\beta + b^2/4\beta$, and $\beta - \mu^2/4\beta$ against the variable β. Below the value $\beta = \frac{1}{2}|b|$ the function $\beta + b^2/4\beta$ begins to diverge from the line β; below the value $\beta = \frac{1}{2}\mu$ the functions $\beta - \mu^2/4\beta$ becomes negative and diverges from the line β. Thus for small values of the parameter β the real lossy medium and Klein–Gordon focus wave modes oscillate more rapidly, as z varies, along the propagation axis as does the non-lossy localized wave, which behaves more 'plane-wave' like for decreasing values of β. As β becomes large the functions $\beta + b^2/4\beta$ and $\beta - \mu^2/4\beta$ asymptote the line β and consequently all three solutions display

Figure 4

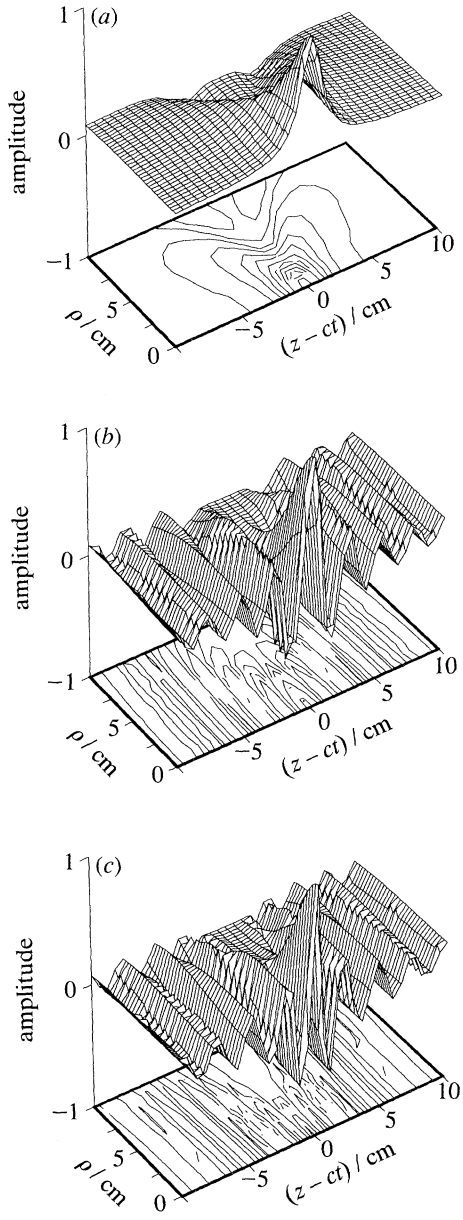

Figure 5

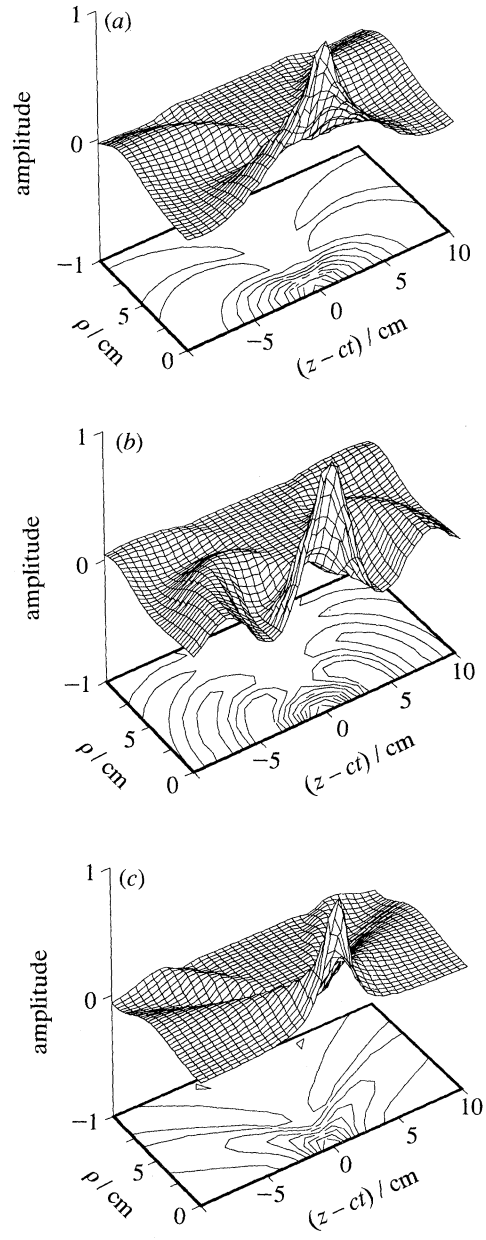

Figure 4 (*a*). $\mathrm{Re}\{\psi_{\beta_{\mathrm{HWE}}}\}(\rho, z, 0)$, (*b*) $\mathrm{Re}\{\psi_{\beta_{\mathrm{LMWE}}}\}(\rho, z, 0)$ and (*c*) $\mathrm{Re}\{\psi_{\beta_{\mathrm{KGE}}}\}(\rho, z, 0)$ surfaces for $0 \leqslant \rho \leqslant 10$ cm and $-10 \leqslant z - ct \leqslant 10$ cm, with $t = 0$. We choose $b = -1$, $\mu = 1$, $z_0 = 1$, and $\beta = 0.1$.

Figure 5. Legend the same as in figure 4, except here $\beta = 0.5$.

essentially the same oscillation along the propagation direction. Again, all three solutions exhibit the same degree of focusing, perpendicular to the propagation axis, as β increases.

This behaviour is shown in figures 4–6. In each figure we have plotted the surfaces corresponding to the real parts of the non-lossy medium, lossy medium, and

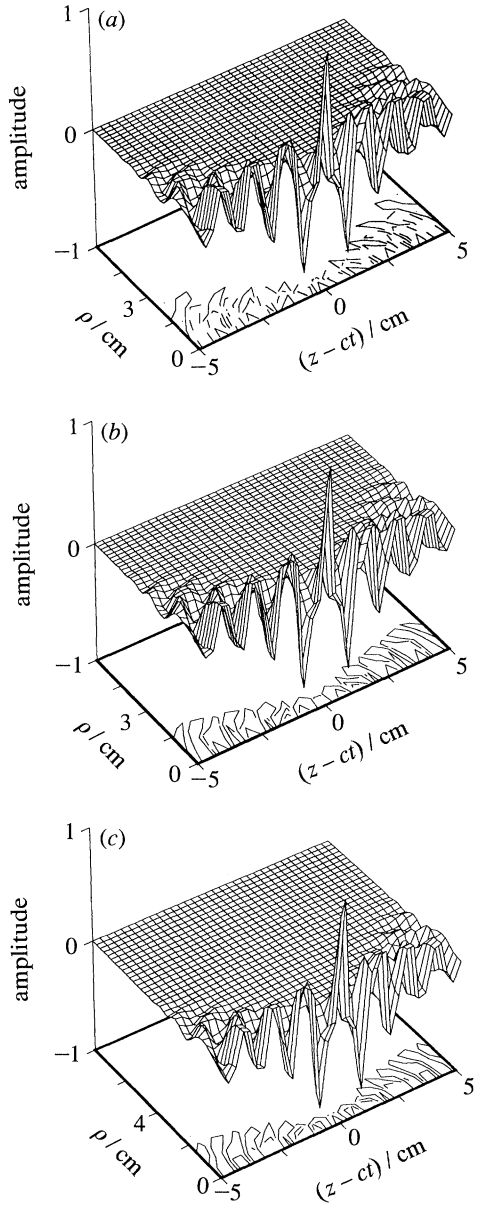

Figure 6. Legend the same as in figure 4, except here $\beta = 5$.

Klein–Gordon LW's as functions of ρ and $z-ct$ (hence ρ and z, as we choose $t = 0$). In each of the three figures we choose $|b| = 1$ for the lossy medium LW, and $\mu = 1$ for the Klein–Gordon LW. Figures 4–6 correspond, respectively, to fixing $\beta = 0.1$, 0.5 and 5 for each of the three LWs. The oscillatory behaviours of the various LWs along the propagation direction, as β changes, is evident.

7. General discussion

The method we have used is based on choosing the Fourier transform of the solution of a homogeneous partial differential equation as a generalized function which, when multiplied by the transform of the differential operator, is zero in the sense of generalized functions. If, for example, we consider the homogeneous wave equation (1), then its Fourier transform is given in (3), which we reproduce here:

$$(k^2-\omega^2/c^2)\,\mathscr{F}_{r,t}\{\psi\}(\boldsymbol{k},\omega)=0. \tag{59}$$

To get the non-separable LW solution in (17) we coupled the temporal and z spatial transform variables (ω and k_z) to the transverse distance (ρ) transform variable, κ, through the two delta functions in (14). A more general solution of (56) is given by

$$f(\boldsymbol{k},\omega)\,\delta(g(\boldsymbol{k},\omega)), \tag{60}$$

where $g(\boldsymbol{k},\omega)$ is a function which is zero only on (possibly part of) the surface $k^2=\omega^2/c^2$ in k_x, k_y, k_z, ω space. In the case of the localized wave solution, whose Fourier transform is given in (14), we see that the support of the delta function in (57), i.e. those points where $g(\boldsymbol{k},\omega)$ is zero, consists of the intersection of the surfaces

$$k_z=\beta-\kappa^2/4\beta \quad \text{and} \quad \omega=-c(\beta+\kappa^2/4\beta). \tag{61}$$

If we consider the three-dimensional half-space $-\infty<k_z,\omega<\infty$, $\kappa\geqslant 0$, the surfaces in (58) represent to 'half parabolic' sheets at right angles. Their intersection line lies on the surface $\kappa^2+k_z^2-\omega^2/c^2=0$. The function $\exp(-\kappa^2 z_0/4\beta)$ in (14) was chosen so that the inverse Fourier transform could be evaluated; it is responsible for the gaussian decay of the space-time solution perpendicular to the axis of propagation.

Although this method makes the localized wave solutions seem natural, what is needed is a greater understanding of how choices of $g(\boldsymbol{k},\omega)$ and $f(\boldsymbol{k},\omega)$ in (57) affect the space-time behaviour of the solution. With this understanding it will be possible to 'design' solutions (for launching) with desired characteristics. We have not attempted to study this more general problem in this paper. Rather, we have contented ourselves with showing how relatively simple transform domain manipulations can lead to the intricate, non-separable, localized wave solutions in space-time. The experiments conducted to launch superpositions of the localized wave solutions (outlined in the Appendix) have all relied on having an explicit expression for the space-time superposition. However, perhaps this is not necessary. Once the transform domain representation for the solution is chosen, whether or not the inverse transform can be evaluated in close form, if we can find (or at least approximate) the temporal Fourier transform of the solution (as we did, for example, in (21)) it may be possible to design passive or active filters whose frequency responses will guarantee the necessary space-time behaviour of the solution; that is to say, transform domain synthesis may be all that is necessary. For example, this might include some type of converter which could take a pulsed gaussian beam and transform it into a beam exhibiting the localized wave properties. On the other hand, perhaps some modulator could be designed to extract the necessary time signal components of a localized wave from one of the new ultrafast pulse sources, such as the photoconductive switches now under development by many groups. Of course, this is where a greater understanding of the duality between transform and space-time domain properties becomes crucial. However, in future experiments to launch various types of acoustic and electromagnetic localized waves these considerations may be important.

In attempting to launch superpositions of the LW solutions, one must be careful that the weighting (spectrum) leads to superpositions with finite total energy. As we saw in §2, a superpositions of LW solutions of the homogeneous wave equation with spectrum $F(\beta)$ will have finite total energy if

$$\int_0^\infty \mathrm{d}\beta |F(\beta)|^2/\beta$$

is finite. Although a similar analysis can be applied to lossy medium LW superpositions, the working is more involved and so here we merely give the result: a superposition of lossy medium LWs will have finite energy if the spectrum satisfies

$$\int_0^\infty \mathrm{d}\beta \frac{\beta}{|\beta^2 - b^2|} |F(\beta)|^2 < \infty. \tag{62}$$

If we compare this constraint with the non-lossy medium one, we see that the lossy-medium spectrum can have larger growth as $\beta \to 0$, but its behaviour is more severely restricted near $\beta = |b| = \mu\sigma c$. A similar analysis can be applied to a superpositions of Klein–Gordon LWs to obtain a constraint on the superposition spectrum.

Appendix A. Localized waves

The homogeneous wave equation (1) has the moving, modified gaussian pulse (Ziolkowski 1985, 1989)

$$\psi_\beta(\boldsymbol{r}, t) = \mathrm{e}^{\mathrm{i}\beta(z+ct)}\, \mathrm{e}^{-\beta\rho^2/V}/4\pi\mathrm{i}V \tag{A 1}$$

as an exact solution. This is the scalar counterpart of the original FWM. The complex variance $1/V = 1/A - \mathrm{i}/R$ yields the beam spread $A = z_0 + \tau^2/z_0$, the phase front curvature $R = \tau + z_0^2/\tau$, and beam waist $W = (A/\beta)^{\frac{1}{2}}$. Because it can be associated with a source at a moving complex location ($\rho = 0$, $z = ct + \mathrm{i}z_0$), (A 1) represents a generalization of earlier work by Deschamps (1971) and Felsen (1976) describing gaussian beams as fields radiated from stationary complex-source points. None the less, the solution (A 1) is source-free in real space. One usually specifies the real part of (A1) as the desired field since the resulting function has its maximum at ($\rho = 0$, $z = ct$). These results are also related to earlier work by Trautman (1962), who considered constructing new solutions of the wave equation by applying complex, inhomogeneous Lorentz transformations to known wave equation solutions. Referring to the Fourier transform (21), the parameter β is free and represents the lowest radian frequency $|\omega_{\min}| = \beta c$ contained in the solution, i.e. the plane wave term in (A 1) acts like a high-pass frequency filter. Similarly, the parameter $|\omega_{\max}| = c/z_0$ defines the $1/e$ roll-off point in spectrum of the solution, i.e. it represents the maximum radian frequency in the spectrum.

The fundamental gaussian pulses (A 1) have either a transverse plane wave or a particle-like character depending on whether β is small or large (Ziolkowski 1989). Moreover, for all β they share with plane waves the property of having finite energy density but infinite total energy. However, as with plane waves, this is not to be considered as a drawback. The above solution procedure has introduced an added degree of freedom into the solution through the variable β that can be exploited, and these fundamental gaussian pulse fields can be used as basis functions to represent new transient solutions of (1).

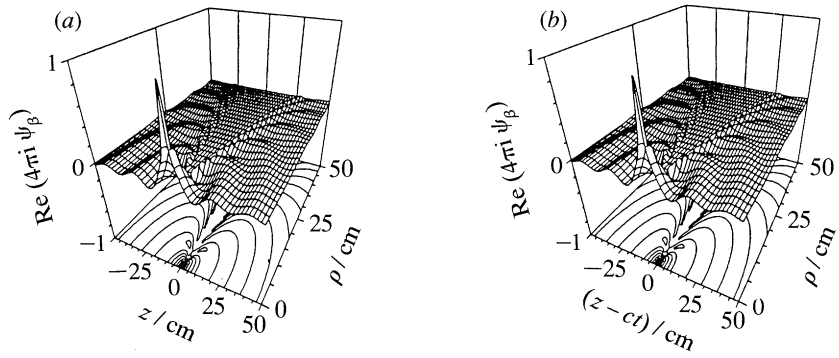

Figure 7. The exact solution ψ_β is a moving, modified gaussian pulse. The real part of $4\pi i\psi_\beta$ for the parameters $\beta = 0.333\ \mathrm{cm}^{-1}$ and $z_0 = 1.0\ \mathrm{cm}^{-1}$ shows the recovery of the initial pulse at a large distance from its initial position. Pulse centre at (*a*) 0 km, (*b*) 942 km.

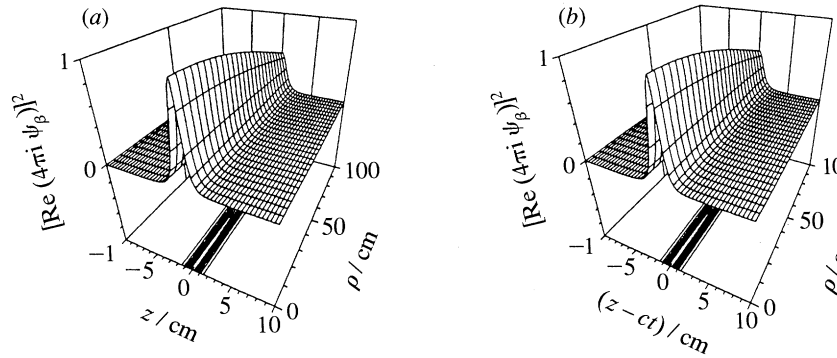

Figure 8. For small values of β the fundamental gaussian pulse looks locally like a transverse plane wave. The square of the real part of $4\pi i\psi_\beta$ is shown for the parameters $\beta = 3.333 \times 10^{-5}\ \mathrm{cm}^{-1}$ and $z_0 = 1.0\ \mathrm{cm}^{-1}$.

As illustrated in figure 7, the HWE solution (A 1) describes a gaussian beam that translates through space-time with only local variations. Figure 7 shows surface plots and the corresponding contours plots of $\mathrm{Re}\{4\pi i\psi_\beta(\rho, z, t)\}$ with $z_0 = 1.0$ cm and $\beta = 0.333\ \mathrm{cm}^{-1}$. These plots depict this quantity relative to the pulse centre locations $z = 0.0$ km and $z = 9.42 \times 10^2$ km. Those distances correspond to the times $t = 0$ and $t = \pi \times 10^{-3}$ s. All of the field quantities plotted in this figure and in figures 8–10 are normalized to their maximum value at $t = 0$ and the direction of propagation is taken along the positive z-axis. These choices do not affect the generality of the following results. The transverse space coordinate ρ is measured in centimetres; the longitudinal space coordinate, $z - ct$, is the distance in centimetres along the direction of propagation away from the pulse centre $z = ct$.

The fundamental gaussian pulses have several interesting characteristics. First, it is easily seen that (A 1) recovers its initial amplitude at very large distances from its initial position. In particular,

$$\mathrm{Re}\,[4\pi i z_0\,\psi_\beta(\rho = 0.0, z = ct)] = \cos(2\beta z),$$

so that its initial amplitude is recovered for every $z = n\pi/\beta$, n being a positive integer. The times in figure 7 were chosen to illustrate this behaviour. Secondly, with z_0 fixed, the pulse becomes more localized with increasing values of β. This effect is

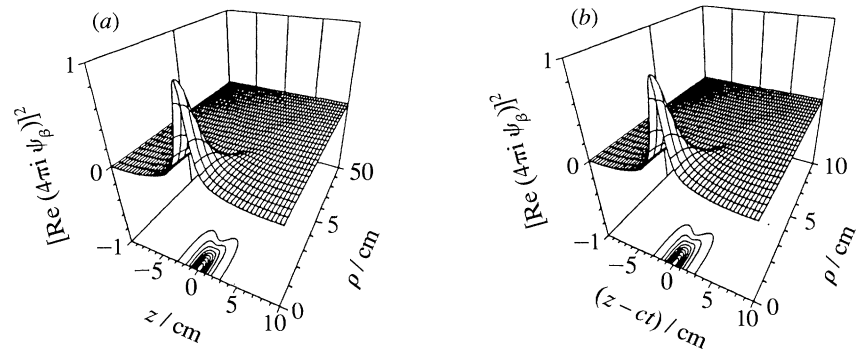

Figure 9. As β increases, the fundamental gaussian pulse becomes more localized along the direction of propagation. The square of the real part of $4\pi i\psi_\beta$ is shown for the parameters $\beta = 3.333 \times 10^{-1}$ cm^{-1} and $z_0 = 1.0$ cm^{-1}.

illustrated in figures 8–10 where $[\mathrm{Re}\,(4\pi i\psi_\beta)]^2$ is plotted. Note that the scales of the axes have been varied to ensure adequate visualization of the major features of this quantity. The parameter β is increased from 3.333×10^{-5} cm^{-1} in figure 8 to 0.333 cm^{-1} in figure 9 to 3.333 cm^{-1} in figure 10. These figures illustrate that for low values of β the HWE solution (A 1) looks like a transverse plane wave locally and that for large β it becomes localized near the z-axis, the axis of propagation. Finally, for all β the fundamental gaussian pulses share with plane waves the property of having infinite energy, but finite energy density. The infinite energy results because the variation of the magnitude of (A 1) with respect to the transverse coordinate yields a constant for each partial energy integral over a transverse cross section. However, as with plane waves, this is not to be considered as a drawback. The form of the solution (A 1) has introduced an added degree of freedom into the solution through the variable β that can be exploited. As shown in Ziolkowski (1989) these fundamental gaussian pulses can be used as basis functions to represent new transient solutions of (1).

Solutions to Maxwell's equations follow naturally from the scalar wave equation solutions. Let f be a LW solution of the scalar wave equation (1). Defining the electric, $\boldsymbol{\Pi}_e = f\hat{\boldsymbol{n}}$, or magnetic, $\boldsymbol{\Pi}_h = f\hat{\boldsymbol{n}}$, Hertz potential along the arbitrary direction $\hat{\boldsymbol{n}}$, one readily obtains fields satisfying Maxwell's equations that are TE or TM with respect to $\hat{\boldsymbol{n}}$. For instance, if a TE polarized field is desired,

$$\left.\begin{aligned} \boldsymbol{E} &= -Z_0 \nabla \times \partial_{ct} \boldsymbol{\Pi}_h, \\ \boldsymbol{H} &= \nabla(\nabla \cdot \boldsymbol{\Pi}_h) - \partial_{ct}^2 \boldsymbol{\Pi}_h, \end{aligned}\right\} \tag{A 2}$$

where $Z_0 = \sqrt{(\mu_0/\epsilon_0)}$ and $Y_0 = \sqrt{(\epsilon_0/\mu_0)}$ are respectively the free-space impedance and admittance.

(a) LW *transmission experiments*

The physics behind the LW effect is the coupling of the usually disjoint portions of phase space: space and frequency, due to the non-separable nature of the LW solutions. The component waveforms, and, therefore, their broad bandwidth spectra, are strongly correlated to each other, a self-similarity property inherent to the LW solution. This means that at any observation point one has different pulses arriving from different locations with different, but correlated, frequency content; i.e. the component waveforms arrive at the right place at the right time with the frequency components necessary to reconstruct the wave packet. A moving interference pattern

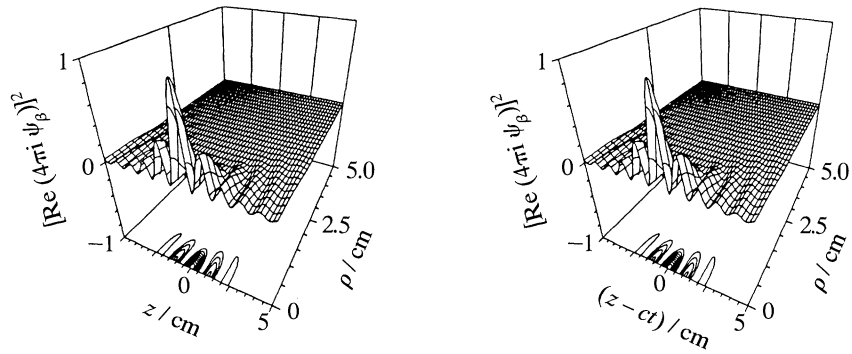

Figure 10. For large β, the fundamental gaussian pulse is very localized along the direction of propagation. The square of the real part of $4\pi i\psi_\beta$ is shown for the parameters $\beta = 3.333\ \mathrm{cm}^{-1}$ and $z_0 = 1.0\ \mathrm{cm}^{-1}$.

forms at enhanced distances as the individual waveforms continue to propagate away from their sources. From a practical point of view, a new type of array is necessary to achieve this effect; each array element must be independently addressable so that the appropriate waveform can be radiated from it.

The LW effect has been verified with a set of three acoustic experiments using ultrasound in water. The first set of acoustic experiments in water was reported by Ziolkowski *et al.* (1989). Successful localization of a transient, pencil-beam of ultrasound launched from a LW pulse-driven array was exhibited. The array was linear, synthetic, and driven with the modified power spectrum (MPS) pulse. The next set of experiments simply extended the previous results to circular and square synthetic arrays. In both cases the pencil-beam generated by the LW pulse-driven array outperformed the corresponding beam transmitted by an array driven with a continuous wave (CW) tone burst. This was true when the array was uniformly illuminated (an effective piston which produces a naturally focused beam) and when it was shaded with a spatial gaussian taper (an initial transverse gaussian with the same waist as the MPS pulse). The beam quality was better than the highest frequency gaussian tested and avoided the inherent near-field variations associated with a piston generated field.

The final experimental series involved an actual array of ultrasonic transducers. This experiment was designed to avoid some of the ambiguities that arise in comparing LW and CW driven arrays. In particular, the LW solutions are composed of broad bandwidth waveforms while traditional performance criteria are based upon CW, narrowband concepts. There is no special frequency that can be selected to define, for instance, a Rayleigh distance when several different broadband spectra are involved. Nevertheless, performance comparisons are desirable and a specific Rayleigh distance L_R was derived for these comparisons (Ziolkowski & Lewis 1990).

A 25-element, 5×5, square array was fabricated which is 1.05 cm on a side and has 0.5 mm diameter disc elements (acoustic transducers) spaced on 2.5 mm centres. The small number of elements limits the number of CW configurations; there are too few elements for any effective shading or focusing. Six unique waveforms were designed for this array to achieve a 10-fold experiment; i.e. maintaining localization at least to $10 \times L_\mathrm{R}$. For the maximum frequency of significance included in these signals, $L_\mathrm{R} \approx 2$–3 cm. The signal design was accomplished with a numerical simulation of the experiment which accounted for the effects (time derivatives of the signals) of the

receiving transducer as well as those of the transmitting ones. Although the resulting time derivatives have no effect on a CW field other than multiplication by a constant, they greatly influence the result of the LW fields because of the inherent correlation between the spectra associated with the spatially distributed set of time signals (an effective coupling of space and time). Comparisons of the energy efficiency (energy received relative to the energy delivered to the array) and beam profile (half width at half maximum of the intensity profile) were made and confirmed more than a 10-fold enhancement of the Rayleigh distance of the beam. As in the synthetic array experiments, the pencil-beam generated by the LW pulse-driven array outperformed the corresponding beam transmitted by an array driven with an equivalent CW tone burst. The sidelobe levels of the LW pencil beam were greatly reduced, especially when compared to beams exhibiting grating lobes which are generated by driving this sparse array with much higher frequency CW tone bursts. The LW pencil beam is quite robust even with a variety of losses and perturbations inherent in the experimental apparatus. Recent analytical results (Ziolkowski 1992*a*, *b*) have extended the meaning of diffraction lengths for the radiated and measured field energies and intensities and of the transverse widths of these beam quantities to the broad bandwidth cases associated with these localized wave pulse-driven arrays. The theoretical and experimental results are in excellent agreement.

This work was done when R.D. was a Visiting Scholar in the Department of Electrical and Computer Engineering at the University of Arizona, during the autumn of 1990. This work was supported by the Canadian Natural Sciences and Engineering Research Council Operating Grant OGPIN 011.

References

Besieris, I. M., Shaarawi, A. M. & Ziolkowski, R. W. 1989 A bidirectional traveling plane wave representation of exact solutions of the scalar wave equation. *J. math. Phys.* **30**, 1254.

Deschamps, G. A. 1971 Gaussian beam as a bundle of complex rays. *Electron. Lett.* **7**, 684.

Felsen, L. B. 1976 Complex-source-point solutions of the field equations and their relation to the propagation and scattering of Gaussian beams. *Symp. Math.* **18**, 39.

Gradshteyn, I. S. & Ryzhik, I. M. 1980 *Table of integrals, series, and products.* San Diego: Academic Press.

Trautman, A. 1962 Analytic solutions of Lorentz-invariant linear equations. *Proc. R. Soc. Lond.* A **170**, 326.

Ziolkowski, R. W. 1985 Exact solutions of the wave equation with complex source locations. *J. math. Phys.* **26**, 861.

Ziolkowski, R. W. 1989 Localized transmission of electromagnetic energy. *Phys. Rev.* A **39**, 2005.

Ziolkowski, R. W., Lewis, D. K. & Cook, B. D. 1989 Experimental verification of the localized wave transmission effect. *Phys. Rev. Lett.* **62**, 147.

Ziolkowski, R. W. & Lewis, D. K. 1990 Verification of the localized wave transmission effect. *J. appl. Phys.* **68**, 6083.

Ziolkowski, R. W. 1992*a* Localized wave transmission physics and engineering. *Phys. Rev.* A. (In the press.)

Ziolkowski, R. W. 1992*b* Properties of electromagnetic beams generated by ultra-wide bandwidth pulse-driven arrays. *IEEE Trans. Ant. Prop.* (Submitted.)

Received 4 October 1991; accepted 21 January 1992